Internal tide modelling and the influence of wind effects.

P. Hall *, A.M. Davies
Proudman Oceanographic Laboratory, 6 Brownlow Street, Liverpool L3 5DA, UK.

Abstract

Initially the development of shallow sea three-dimensional barotropic tidal models is briefly reviewed with a view to determining what were the key measurements that allowed progress in this field and rigorous model validation. Subsequently this is extended to a brief review of baroclinic tidal models to try to determine a way forward for baroclinic model development. The difficulty of high spatial variability, and wind influence are identified as possibly important issues that must be considered in validating baroclinic tidal models. These are examined using a three-dimensional unstructured grid model of the M_2 internal tide on the shelf edge region off the west coast of Scotland. The model is used to investigate the spatial variability of the M_2 internal tide, and associated turbulence energy and mixing in the region. Initial calculations are performed with tidal forcing only, with subsequent calculations briefly examining how the tidal distribution is modified by down-welling and up-welling favourable winds. Calculations with tidal forcing only, show that there is significant spatial variability in the internal tide and associated mixing in the region. In addition, these are influenced by wind effects which may have to be taken into account in any model validation exercise. The paper ends by discussing the comprehensive nature of data sets that need to be collected to validate internal tidal models to the same level currently attained with three dimensional barotropic tidal models.

1. INTRODUCTION

In the context of this volume concerned with reviewing developments in hydrodynamic modelling, and presenting new results that point to the way forward, we consider the topic of accurately computing internal tides and how they are modified by wind effects. In addition, the extent to which this influences model/data comparison is considered. In this introduction we initially very briefly review the major stages in the history of how finite difference and finite element modelling of tides has developed in shallow sea regions. This development has now progressed to such an extent that in shallow sea regions, models can be used to give accurate real time predictions of currents for navigation purposes (e.g. Gjevik et al., 2006). The main aim of this overview is to understand what has in the past limited progress and how it was overcome. From this the present limitations of models of the internal tide in shelf edge regions can be understood and suggestions for a way forward developed. Based on this and the modelling presented here, in the conclusions we try to suggest the extent and nature of new measurements required to validate internal tide modelling and progress that field.

Initially, research on tidal modelling was confined to shallow sea regions and the application of, by todays standards, relatively coarse grids using finite difference methods. In particular, the Arakawa C grid was used in these calculations. The main emphasis in these models was the determination of tidal elevation for the major component of the tide, namely the M_2 constituent. Since elevations rather than currents were the primary focus, the two-dimensional vertically integrated equations could be used, thereby reducing computational effort. In Europe the main emphasis was on the North Sea, although as computational resources increased the north-west European Shelf became the primary focus as it covered a range of water depths and tidal regions. In addition some areas, such as the Bristol Channel had an enhanced tidal range due to resonance. An early example of a successful simulation of the M_2 tide over the European shelf is given in Flather (1976). His shelf wide model had an open boundary at the shelf edge which was specifically designed to use measurements of Cartwright (1976) in the shelf edge region. By this means an accurate tidal forc-

* Corresponding author.
Email address: phh@pol.ac.uk (P. Hall).

Postprint of article published in Continental Shelf Research (2007) 27: 1357–1377 *18 July 2007*

ing was introduced along the open boundary of the model. This was of course a key factor that progressed the modelling. Although the model grid was coarse, of order 30km, the model could reproduce the propagation of the tide from the shelf edge into the interior of the region. However, the lack of resolution meant that some regions such as the English Channel were poorly resolved, and the generation of higher harmonics in near coastal regions could not be reproduced. In essence this model could reproduce the main features (co-tidal chart) of the M_2 tide in regions where a 30 km resolution was adequate. However, close to the coast where the tide changed rapidly over short distances (of order 10 km) and higher harmonics were generated the models accuracy rapidly degraded.

In order to examine the accuracy of this type of finite difference or finite element model in nearshore regions limited area high resolution models were used (e.g. Walters (1987); Walters and Werner (1989); Werner (1995), also review in Walters (2005)). In such fine grid models in regions of large tidal amplitude, wetting and drying occurred during the tidal cycle and finite difference and finite element codes were modified to take account of this (e.g. Flather and Hubbert (1989); Fortunato et al. (1997, 1999); Heniche et al. (2000); Ip et al. (1998)). This gave rise to a significant increase in accuracy of both the fundamental and higher harmonics of the tide. Recently, inverse modelling methods (e.g. Thompson and Griffin (1998); Chen and Mellor (1999); Lynch and Hannah (2001); Lynch et al. (2004)) have been developed whereby coastal data is assimilated into a limited area model in order to improve the accuracy of the tidal solution. However, as shown by Lynch et al. (2004) in order to obtain an accurate solution over the whole region it is essential to accurately represent the nearshore region where observational data is assimilated. If this is not done then an erroneous inverse is generated and an inaccurate tidal solution is produced. The paper by Lynch et al. (2004) clearly shows that it is essential to resolve the physics and topography in the region of strong tidal signals, namely the coastline in the case of a barotropic shelf tidal model.

In parallel with these developments in shallow sea modelling, basin wide tidal modelling with coarse grids was also progressing. These models included the tide generating forces, and hence the tide was not forced as a co-oscillating tide through the open boundary as in a limited area coastal model. However, since the grid was coarse they could not resolve the shelf sea regions where dissipation occurred. Consequently, in these basin wide models energy was lost by radiating through the open boundary which was effectively at the shelf edge. Recently, the ability to improve resolution in these regions and the use of altimetry with data assimilation has led to significant progress in the accuracy of barotropic ocean tidal models (e.g. Shum et al. (1997)). Another recent example of inverse oceanic tidal modelling that uses TOPEX/Poseidon data with an efficient inverse method is given in Egbert and Erofeeva (2002). However, the topic of data assimilation is beyond the scope of this paper, but references and discussion are given in a recent paper by Thompson et al. (2007).

With increasing computing power three-dimensional models have been developed, and more complex unstructured grid methods have been established. The designing of optimal grids and associated issues relating to accurately computing the tide in a range of environments, from ocean, across the shelf edge and into the nearshore region has been a topic of significant research in recent years. It has led to the development of a range of considerations that should be borne in mind in the design of time independent grids (e.g. Legrand et al. (2007); Greenberg et al. (2007)), and time evolving unstructured grids (e.g. the review by Pain et al. (2005)).

In shallow sea regions where tidal mixing is strong and the water column remains well mixed then stratification effects upon tidal turbulence are absent. Consequently, although tidal currents over a region may have been collected at different times, the periodic nature of the tides means that in essence a synoptic data set can be produced. This involves harmonic analysis, giving amplitude and phase which can be added to an existing database from earlier observations thereby enhancing its accuracy and spatial coverage. However, in stratified regions, in particular those adjacent to topography (e.g. Dogger Bank, Proctor and James (1996)) where stratification changes and internal tides are generated, the problem is more complex and a synoptic set of tidal and associated density fields is required.

The significant spatial change in topography and density field in the shelf edge region (Pingree and New (1991)), gives rise to a high degree of spatial variability in the internal tide (e.g. Pingree and New (1989, 1995)), this together with the influence of the wind upon stratification and hence the internal tide (Xing and Davies (1997b) (hereafter XD97)) makes the collection of accurate and comprehensive data sets in these regions particularly difficult. Hence, data sets for a rigorous skill assessment of internal tide models are very difficult to obtain. Despite these difficulties significant progress has been made using numerical models to improve our understanding of internal tide generation and propagation. Early models used primarily analytical approaches (Craig (1987); Sherwin and Taylor (1989, 1990)) and were of cross-sectional form. Although numerical models (e.g. Holloway (1996); Xing and Davies (1996a,c), hereafter XD96a, b; Xing and Davies (1997a)) in cross-sectional form were also used. Subsequently three dimensional models were developed (e.g. Cummins and Oey (1997); Niwa and Hibiya (2004); Merrifield and Holloway (2002); Simmons et al. (2004); Munroe and Lamb (2005)) and used to examine the generation of the internal tide in a range of geographical locations. These models were able to extend the results from the cross sectional models, and showed the importance of along shelf topography (which recent observations (Sherwin et al. (2002)) have shown to have a significant effect on the tide), off shelf seamounts (Xing and Davies (1998b), hereafter XD98; Xing and Davies (1999)), and how the shape of shelf slopes, seamounts and ridges influenced internal tide propagation (Holloway and Mer-

rifield (1999); St. Laurent et al. (2003); Cummins et al. (2001); Hibiya (2004)). However, the hydrostatic nature of these models meant that soliton generation and propagation could not be included. To examine these, a range of models that solved the KdV equations was developed and proved very successful in determining the processes leading to soliton generation at the shelf edge (e.g. Gerkema and Zimmerman (1995); Gerkema (2001, 2002)).

With enhanced computational resources the solution of the non-hydrostatic equations (e.g. Adcroft et al. (1997); Marshall et al. (1997b,a); Berntsen and Furnes (2005); Berntsen et al. (2006)) in cross-sectional form was possible, giving rise to detailed studies of soliton development at the shelf edge (Lamb (1994, 2002)). In addition, this form of model was used to examine the generation of higher harmonics of the tide in the proximity of seamounts (Lamb (2004)), and the extent to which energy is radiated as internal waves (Lamb (2007)).

The degree to which tidal barotropic energy at the shelf edge or in other regions of abrupt topography is partitioned between internal waves which can radiate energy away from the region, or local mixing is a topic of increasing importance. To get the correct form of energy transfer from the barotropic tide to the baroclinic tide, higher harmonics (Khatiwala (2003)) and short waves that contribute to mixing it is essential to use a non-hydrostatic model (Xing and Davies (2006)). Also the problem of tidal mixing in shelf edge regions of rough topography has been investigated (e.g. New (1988)). This enhanced mixing has been shown to have important consequences for the computed circulation produced by large scale models (e.g. Samelson (1998); Spall (2001)). Recently (Saenko and Merrifield (2005); Saenko (2006)), this work has been extended, particularly in Saenko (2006) where a coupled ocean-atmosphere model with various vertical diffusivity distributions was used to determine the sensitivity of the solution to these distributions. Calculations showed that climate models gave different meridional oceanic circulations, heat transports, stratification and climate response to atmospheric CO_2 increase depending upon whether vertical diffusivity was or was not related to spatial variations in internal tidal mixing.

This suggests that the accuracy of climate models will be significantly influenced by the ability of the oceanic model to accurately reproduce the intensity and spatial variability of mixing due to the internal tide. To examine this mixing in detail, and in particular the consequences of along slope rough topography, three dimensional non-hydrostatic calculations have been performed (Legg and Adcroft (2003); Legg (2004b,a)).

To date the majority of these calculations used uniform finite difference models, or models with an across shelf grid refinement. However, as clearly demonstrated by the shallow sea applications of finite element models, this approach is ideal in a shelf edge environment where both enhanced resolution is required at the shelf edge and at offshore locations e.g. seamounts.

The advantages of using finite elements to compute the M_2 component of the internal tide in a shelf edge region with off shelf seamounts was examined by Hall and Davies (2005a), (hereafter referenced as HD05a). To make a comparison with a fine resolution (2.4 km across shelf and 4.6km along shelf) finite difference internal tide model, (XD98), HD05a used a range of finite element meshes to compute the internal tide off the west coast of Scotland. The region covered by the model, namely the Malin-Hebrides shelf, was identical to that used by XD98, as were the open boundary conditions and water depths. Also the same vertical stratification was used. By this means a like with like comparison was possible and the influence of finite element resolution on the internal tide could be determined. A comparison with limited measurements (although not all collected under identical conditions) was also possible. Although the main features of the internal tide computed with the finite difference model and the coarse and fine finite element model were comparable, it was evident that the intensity of the M_2 internal tide in its generation region and its subsequent propagation was improved by using the finer mesh finite element grid. However, no appreciable improvement in comparison with observations was found, presumably because of slight differences in stratification between the model and those taken at the time of the measurements. In addition, as shown by Xing and Davies (1997b) using a cross sectional model with idealized topography, meteorological effects can influence the distribution of the internal tide. As no measurements of meteorological forcing or its effect upon the stratification at the time the internal tide measurements were made it is not possible to quantify from the measurements the extent to which the internal tide is influenced by meteorological forcing. Consequently, it is not possible to state from existing observations to what extent such measurements are required in order to validate models of the internal tide. However, results from the cross section model of XD97 using idealized topography suggests meteorological effects have a major influence on the internal tide.

In this paper, the work presented in XD97 is extended to the case of a three dimensional model. A finite element rather than a finite difference approach is used. The region considered is the Malin-Hebrides shelf, and the model resolution is identical to that used by HD05a. By comparing differences in the internal tide, produced under a range of wind conditions, some insight as to the role meteorology does or does not play in modifying the internal tidal signal in different regions can be assessed. At locations where the internal tide is particularly sensitive to wind direction, then an assessment as to the value of internal tide measurements in these regions without the associated meteorological forcing, in a model skill assessment can be determined. In essence the aims of the paper are twofold. The first, to understand the role of wind direction in modifying the internal tide in a three-dimensional model. The second to appreciate the sensitivity of internal tide measurements in a given area to small scale variation with and without wind forcing and hence their reliability in any skill assessment

exercise.

The form of the paper is such that the model and region considered is detailed in the next section. Subsequent sections describe the three dimensional variability of the M_2 internal tide. Later the response to wind forcing and the resulting changes in tidal distribution are considered, with a final section summarizing results and presenting a "way forward".

2. The hydrodynamic model and region

Although previous calculations (XD97) used a cross-sectional model, the full three-dimensional equations and the turbulence closure model were presented there and elsewhere (Xing and Davies (2001c)). Consequently, they will not be repeated here, where we will summarize their main features. In addition, to be consistent with XD97, the hydrostatic approximation is used in these equations and density is derived from temperature using a simple equation of state (XD98). The rigid lid approximation is not made, and the model is forced by the barotropic tide. Consequently, the model is fully prognostic, with free surface elevation changing as the tide propagates on and off shelf. This propagation produces up-welling and downwelling of the temperature field in the shelf edge region and hence the generation of an internal tide (XD98, HD05a). Vertical mixing of momentum and density are parameterized using vertical eddy viscosity and diffusivity coefficients computed using a turbulence energy closure, namely Mellor and Yamada sub-model. This sub-model contains predictive equations for length scale and turbulence energy. As the form of the model is given elsewhere (Blumberg and Mellor (1987), pp. 116; Luyten et al. (2002) ; XD98) it will not be repeated here. The Smagorinsky (1963) form of horizontal eddy viscosity has been shown by Hall and Davies (2005c) (hereafter HD05b) to be particularly good at preventing the development of numerical instabilities when wind forced internal waves are generated on an irregular grid. This form of viscosity is used here.

Since the present calculation is concerned with the short term modification of the internal tide due to wind forcing, rather than its seasonal variation, there is no applied surface heat flux. However, wind stress forcing from various directions is used, and incorporated as a surface boundary condition on momentum and turbulence as in XD97. A quadratic friction law as in XD98 was applied at the seabed. Along the open boundary identical barotropic tidal forcing to that used in the finite difference model (XD98) and finite element model (HD05a) was applied. A sigma coordinate with 40 levels in the vertical was used in the calculations. The spacing was such that there was enhanced resolution in the near-bed and near surface region (as in XD98, HD05a) where the internal tide was largest. As in HD05a, the finite element code (QUODDY, Lynch et al. (1996)) was used to solve the discretized hydrodynamic equations.

The shelf and shelf edge region in the finite element model (Fig. 1) is identical to that used by XD98 and HD05a. The area covers a range of water depths from the order of 10m close to the coast to 3000m in the ocean. At the shelf edge (approximately the 200m contour) water depth changes rapidly, as it does along the edge of the Anton Dohrn Seamount and Hebrides Terrace Seamount. As shown in XD98 and HD05a, in these regions there is appreciable internal tide generation. Detailed studies using a range of unstructured grid approaches (HD05b, Hall and Davies (2005b)) showed that to accurately reproduce wind forced internal waves generated in regions of topographic change it was necessary to have a fine grid adjacent to the topography. Similarly, HD05a, found that to reproduce the internal tide in the region shown in Fig. 1, to a greater accuracy than that found in XD98, it was necessary to refine the grid in the regions of rapidly changing topography. To accomplish this the same finite element grid (Fig. 2) used by HD05a, in their tidal calculations is applied here. Ideally a more gradual transition in element size as the shelf edge is approached may be preferable to that shown in Fig. 2. However, this would increase the computational effort, and as shown in HD05a, by comparing various mesh resolutions, and from more idealized calculations (HD05b, Hall and Davies (2005b)), the mesh given in Fig. 2 yields an accurate solution. In addition, by using the same mesh in the present calculations a direct comparison with HD05a is possible, enabling the effect of the wind upon the tide to be determined. As in all calculations that use a sigma coordinate representation in the vertical, there are problems with computing the internal pressure gradient and other terms (e.g. Haney (1991); Mellor et al. (1998)) with such an approach. In regions of steep topography errors in the internal pressure gradient can give rise to a spurious along shelf flow. However, this effect can be minimized by ensuring that as water depth changes so does the horizontal grid resolution, so as to maintain the Haney condition (Haney (1991)). In a region of varying density gradient, water depth and shelf slope, where the finite element grid is often chosen to ensure an accurate representation of the slope region (see Legrand et al. (2007)) the Haney criterion is of necessity violated in a number of regions and hence a small erroneous along shelf flow is generated. In the present calculation the mesh was refined to resolve as accurately as possible the shelf slope topography, but not to such an extent that the departure from the Haney criterion was excessive. In essence the horizontal resolution in the shelf slope region was consistent with that used in the vertical. In addition, the residual flow determined from the harmonic analysis used to derive the M_2 component of the tide did not show a large spurious shelf edge flow (HD05a).

In all calculations the model started from a state of rest with zero elevation and current, with the same temperature profile as used by XD97, applied everywhere. By this means the temperature surfaces were initially horizontal. The M_2 barotropic tidal forcing was applied along the open boundary and as found in HD05a, after 6 tidal cycles a periodic barotropic tide and quasi-periodic baroclinic tide

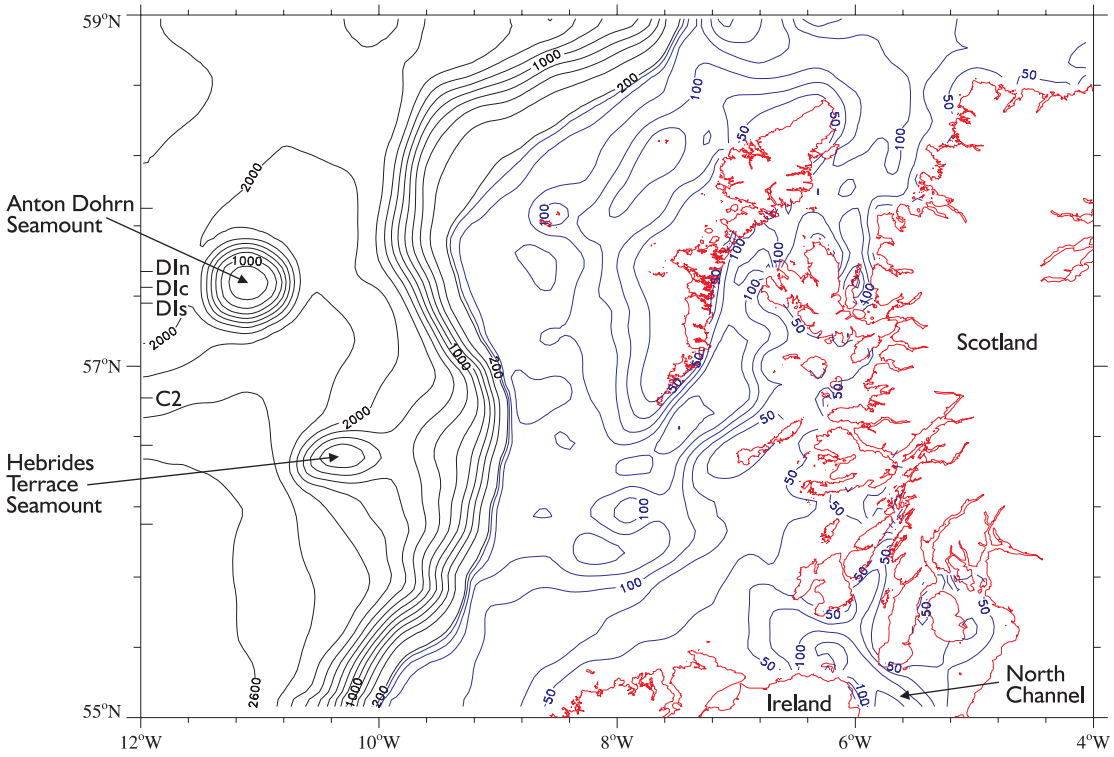

Fig. 1. Model domain and bottom topography (water depths in m) used in the calculations. The lines marked C2, D1n, D1c and D1s denote the latitude of cross sections where the influence of the wind upon the tide is examined in detail. Also shown are geographical locations of regions named in the text.

were established, which was harmonically analysed to give the tidal distributions shown here. Although the western side of the Anton Dohrn seamount is in close proximity to the open boundary this did not pose a major problem as the internal tide was mainly confined to the region of the seamount (see detailed analysis of energy fluxes in XD98).

To be consistent with XD98, only the M_2 internal tide is examined, although the S_2 tide is also appreciable. In addition, the barotropic diurnal tides K_1 and O_1 are intensified in this region due to shelf edge resonance (see Xing and Davies (1998a) for detail). However, as these components are subinertial they do not give rise to an internal tide, but have significant barotropic currents in the region.

In subsequent calculations the effect of wind forcing produced by a uniform steady wind, upon the M_2 tide was examined. To be consistent with XD97, a wind stress of 0.2 Pa was applied. To avoid the generation of strong inertial oscillations which would persist in the solution and mask the steady wind induced response, the wind stress was increased with a sine wave form corresponding to the first quarter of a sine curve (namely 0 to $\pi/2$) for 12 h during the spin up stage.

3. Tidal calculations

In an initial calculation (Calc. 1, Table 1) as in HD05a the model was forced by the barotropic tide. As discussed in HD05a, this produces a strong baroclinic tide that is separated from the total solution by subtracting a barotropic tide computed by running the model in a homogeneous form (see HD05a for detail). The resulting baroclinic tidal cycle is then analysed to yield the M_2 component of the baroclinic tide. A similar approach was applied in the wind forced case.

Calc	Wind duration	Wind magnitude	Wind towards
1		Tide only	
2	Short	0.2Pa	North
3	Long	0.2Pa	North
4	Short	0.2Pa	South
5	Long	0.2Pa	South

Table 1
Summary of various calculations.

As shown by XD96a, b, XD97 and HD05a, the presence of the Anton Dohrn offshore seamount at about 57.5 °N (Fig. 1) influences the distribution of the M_2 internal tide in this region. For this reason we will start by examining the distribution of the M_2 tide in this area, initially without and subsequently with wind forcing. By comparing solutions the influence of wind effects on the M_2 internal tide can be quantified. As shown in HD05a, there is significant spatial variability in the M_2 internal tide in the region of the Anton Dohrn seamount, due to local topographic variations. To examine this variability in the baroclinic tide, cross sections D1n, D1c and D1 s (Fig. 1) are initially con-

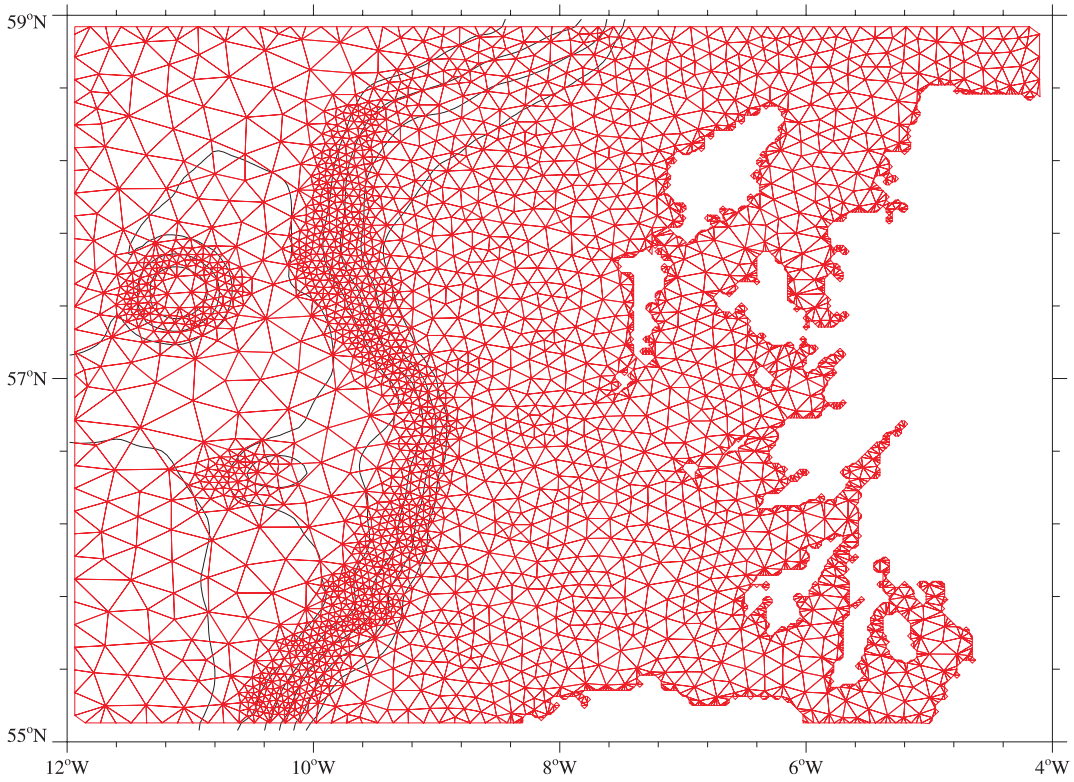

Fig. 2. Finite element grid used in the calculations.

sidered in detail to determine how local changes in topography influence the M_2 tide in the absence of wind forcing. From Figs. 3a-c, it is evident that the large-scale features of the u current amplitude of the internal tide found by XD96 in their finite difference solution are present here. On the shelf a surface and bottom intensification of M_2 baroclinic current amplitude (Fig. 3a) which is indicative of a first mode internal wave is evident at all locations. In addition, the bottom intensification of the internal tide at the shelf break, extending down the slope was also found by XD98. The extent of this downslope region of intensified bottom current does however vary from section to section (compare Figs. 3a-c).

The generation of an M_2 internal tide along the edges of the seamount, with a surface maximum was also found by XD98. However, it is clear from Figs. 3a-c that the intensity and distribution varies significantly in the seamount area. As shown by XD96a, XD98, in the Anton Dohrn region both super-critical and sub-critical internal tides are generated along the shelf slope and on the seamount sides, producing internal tides that propagate both onto the shelf and into the ocean. In both threedimensional calculations with and without the seamount, and two dimensional cross section calculations, XD98 showed that the exact location and topography of the seamount was responsible for the offshelf distribution of the internal tide. At cross section C2, to the south of the seamount, where the slope is steeper, the region of maximum M_2 internal tide occurs down the slope in deeper water (Fig. 3d). A surface intensification is present in the shelf break region, with a slight increase on the shelf at depth. This suggests that there is little on shelf propagation of the internal tide at this cross section.

To determine to what extent tidal mixing, as the internal tide upwells and downwells over the steep topography influences the temperature field, the tidally averaged (over a tidal period) temperature field over cross section D1 was examined (Fig. 4). Temperature contours on the shelf (Fig. 4), show a well-mixed region in shallow coastal waters (to the east of 9.5 °W and not covered in Fig. 4) with a near vertical displacement relative to the topography of isotherms in regions of steep topography. Some of this is due to boundary layer mixing. In addition, advection by residual flows generated by non-linear effects (Xing and Davies (2001b)), and density driven currents produced by differential mixing between lateral boundary layer flow and currents outside the boundary layer also contribute to the displacement of temperature surfaces from their initial positions. Although it is evident from Fig. 4, that the extent of this displacement varies with depths below the surface, it is useful to examine its spatial variability at a given depth. To this end the model was run for a significantly longer period of time (namely 20 tidal cycles) to allow tidal mixing and tidally produced turbulent kinetic energy (t.k.e.) to become established.

A near uniform spatial distribution of temperature at 600m was found away from the Anton Dohrn Seamount and

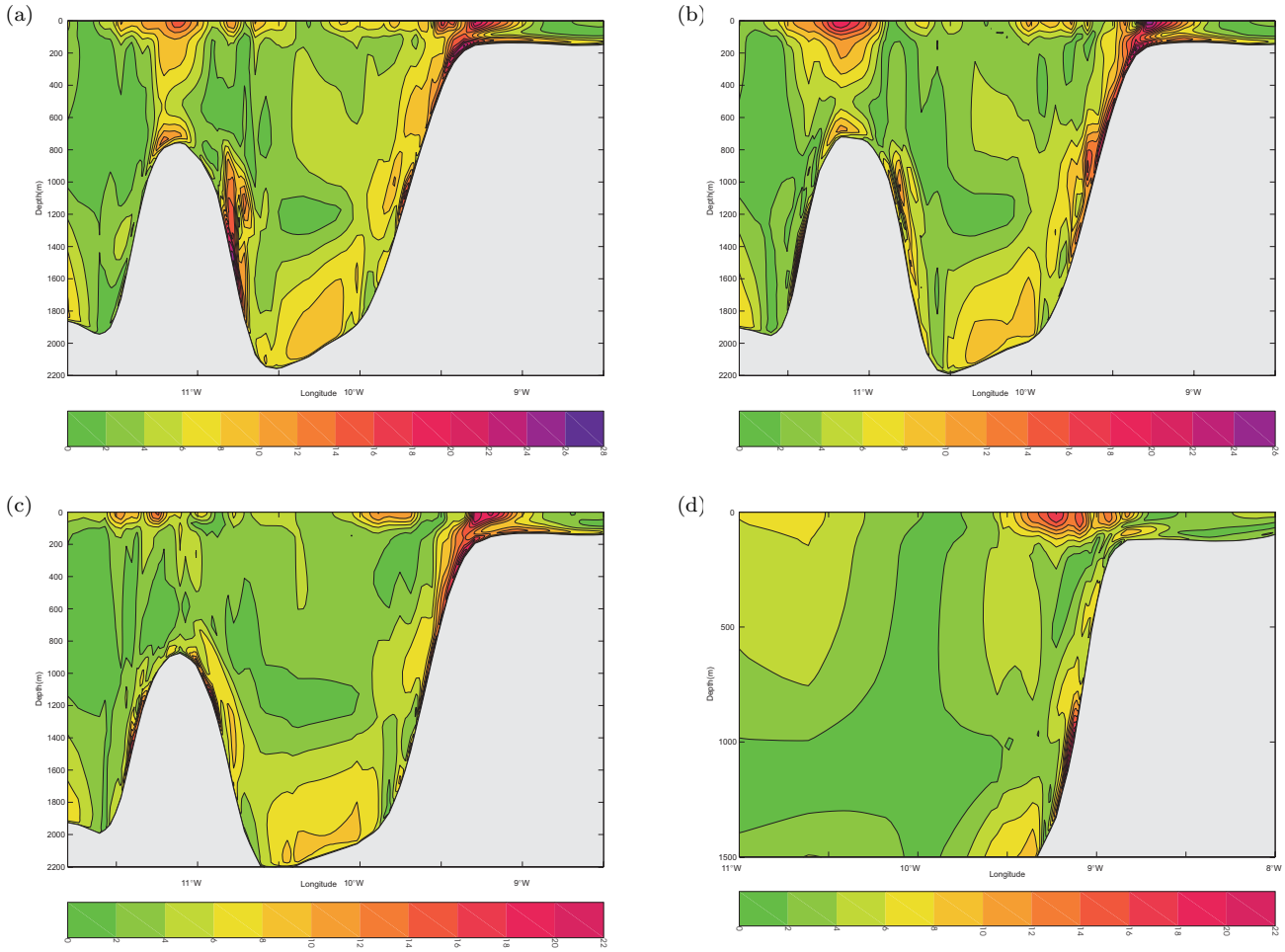

Fig. 3. Amplitude (cm s^{-1}) of the M_2 harmonic of the u-component of the baroclinic tide along various cross sections, namely (a) D1n, (b) D1c, (c) D1s and (d) C2 from a short tidal integration.

the shelf edge region. As this water depth is above the top of the seamount, the reduction in temperature is associated with enhanced vertical mixing above the seamount. The nature of this mixing will be discussed later in the paper. Similarly in the shelf edge region enhanced up-welling and vertical mixing leads to regions of colder water at a depth of 600m in the shelf edge region to the north of 57 °N (Fig. 5). The lateral extent of the cold water region varies along the shelf edge, tending to be largest in the region to the north-east of the Anton Dohrn seamount where there is an appreciable M_2 tidal energy flux both along and across the depth contours (see Fig. 3 in XD98). A comparable energy flux occurs over the Anton Dohrn Seamount (XD98). To the south of 57 °N in the region of cross section C2 there appears to be a region of slightly warmer shelf edge water at 600m depth, compared to the oceanic temperature. In this area, the orientation of the shelf edge relative to the tide is different than farther north (XD98). Also the shelf slope is different (compare shelf edge gradients in Figs. 3b and d) giving rise to a maximum internal tidal current at about 1200m depth (Fig. 3d) rather than higher up the slope (of order 600 m) found farther north (Fig. 3b). These differences in location at depth of maximum internal tidal current generation suggests that there will be differences in shelf slope boundary layer mixing with depth that will influence the temperature distribution, and hence internal tide generation and propagation. A detailed study of the distributions of temperature, turbulent kinetic energy, eddy viscosity and mixing (not presented) showed that regions of maximum t.k.e. occur at locations of maximum internal tidal current amplitude. Consequently, in the shelf slope region there will be considerable small-scale variation in the location of strong t.k.e. regions and associated mixing. This gives rise to significant spatial variability in the internal tide, suggesting that a detailed measurement programme is required for model validation in such areas.

4. Wind influence upon the internal tide

4.1. *A down-welling favourable wind (wind towards the north)*

In this series of calculations, in addition, to barotropic tidal forcing through the open boundary the model was

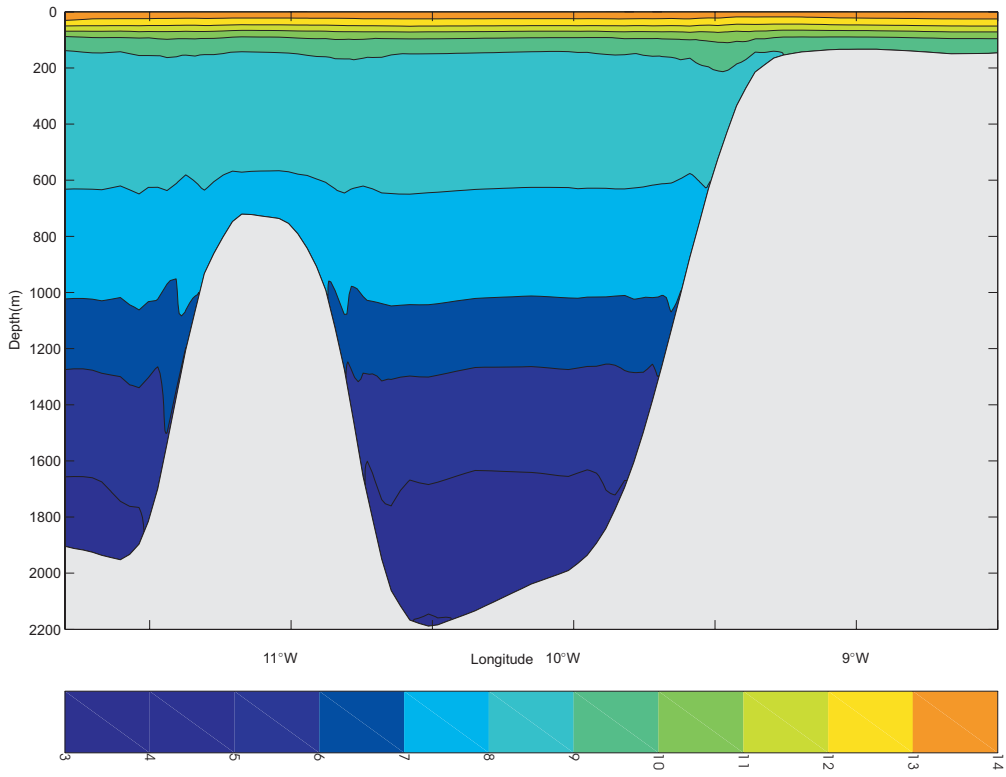

Fig. 4. Temperature contours (°C) at cross section D1n from a short tidal integration.

forced by a down-welling favourable wind (wind towards the north) of 0.2 Pa (Calc 2, Table 1). On the short time scale, time averaged (over an M_2 tidal cycle) temperature contours along cross section D1n (not presented) show some enhanced mixing and weakening of the thermocline in the surface layer (top 100 m), with little or no change at depth. Contours of the difference in u amplitude of the M_2 internal tide show (Fig. 6) that the change in the M_2 internal tide is mainly restricted to the surface layer where the density field has been modified by the wind. The largest changes occur in the surface layer above the seamount and along the shelf edge where the current due to the internal tide was a maximum (Fig. 3a). On average these changes were of the order of 5 cm s^{-1}, (Fig. 6) compared with the M_2 internal tidal current amplitude (Fig. 3a) of order above 20 cm s^{-1}. At other cross sections (not shown) the change in surface temperature field and distribution of the M_2 internal tidal current was not appreciably different to that shown in Figs. 4 and 6.

In this calculation the wind stress was only applied for a short period of time. Consequently, the major change in the density field only occurred in the surface layer. As shown by XD97 in a cross section model, when a wind stress of 0.2 Pa was applied for 30 tidal cycles there was appreciable upwelling along the shelf slope region which affected the generation and offshelf propagation and hence the M_2 tide at depth. To examine this in more detail, particularly in the seamount region the previous calculation was repeated with the wind applied for 20 tidal cycles (Calc. 3).

Contours of the mean temperature at cross section D1n, reveal a significantly weaker surface thermocline (Fig. 7), with appreciably more mixing in shallow water than found in the tide only calculation (Fig. 4). At depth, particularly in the regions adjacent to the sea bed, enhanced mixing has changed the local density gradient. Part of this mixing is due to the wind field, but a plot of temperature contours at the same time without wind showed that because of the extended time integration period tidal mixing had also contributed to the mixing at depth in slope regions.

Contours of the difference in baroclinic M_2 u-current amplitude (Fig. 8) between those computed with long period wind forcing and the equivalent tidal forcing only, show that there is no substantial change on the shelf. However, in the surface layer above the shelf break and at the top of the shelf slope there has been an appreciable change in M_2 baroclinic tidal current amplitude (Fig. 8) associated with the change in stratification in this region. Similarly at depth near the foot of the slope an appreciable M_2 internal tide is produced (Fig. 8) associated with the change in stratification in this region. A strong internal tide is also produced along the western side of the seamount (Fig. 8). Previously (Fig. 3a) there was no internal tidal signal in this region. The reason for the appearance of the internal tide in this region is due to a local change in stratification

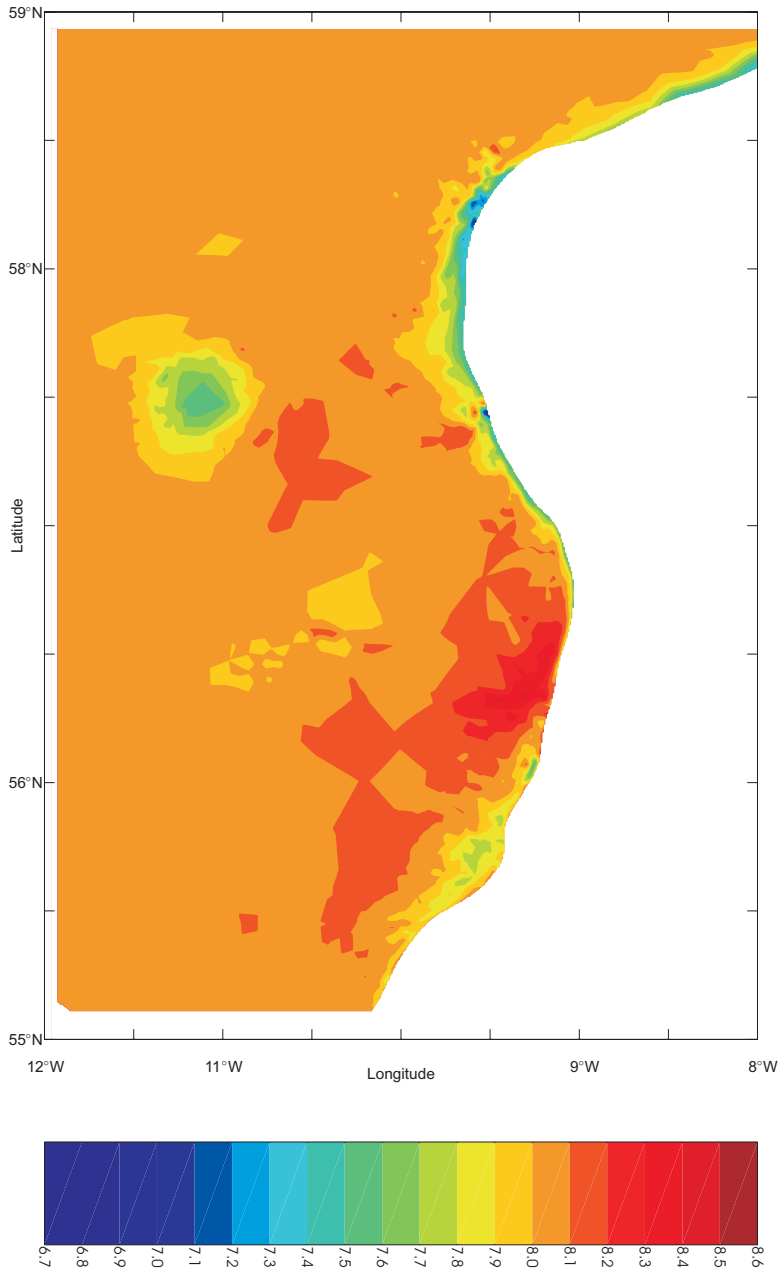

Fig. 5. Horizontal temperature distribution (°C) at a depth of 600m below the surface from a long tidal integration.

due to prolonged tidal and wind induced mixing. A similar change occurred at cross sections D1c and D1s (not shown) due to comparable changes in the stratification at depth.

To determine to what extent the presence of a long (20 tidal cycle) wind stress of 0.2 Pa towards the north has upon the turbulence energy distribution, and mixing a detailed study of the spatial distribution of turbulence and temperature was performed (not presented). This shows that the presence of the surface wind stress gives rise to an enhanced layer of surface and onshelf turbulence at cross

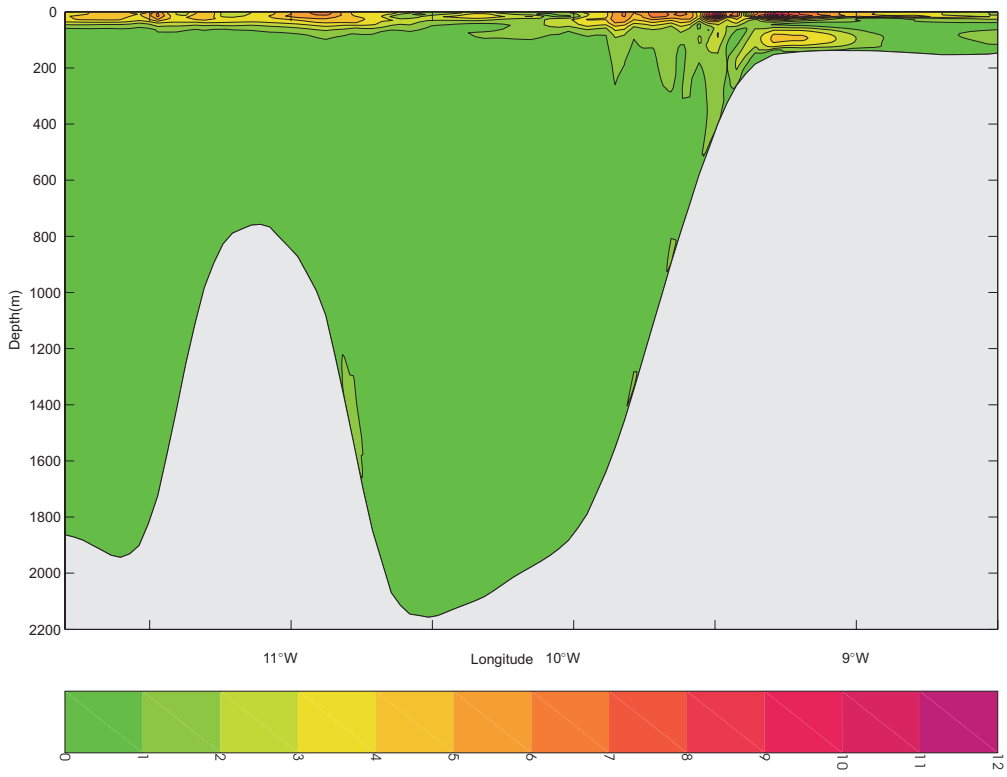

Fig. 6. Contours of the difference in M2 baroclinic tidal amplitude (cm s^{-1}) between the wind (0.2 Pa North) and tidal solution and a tide only solution for short wind duration forcing (Calc. 2) at cross section D1n.

section D1n that was not present with only tidal forcing. In addition, the distribution of t.k.e. in the seamount and shelf slope region changes, associated with wind induced circulation and mixing, and corresponding changes to the density field. Associated with this change in density field are changes in the location and intensity of the internal tide. Similar changes in t.k.e. distribution occur along the other seamount cross sections (not shown), although the spatial variability of the mixing from one cross section to another appears to be enhanced by the presence of the wind.

This series of calculations clearly shows that a modest wind stress of 0.2 Pa can modify the distribution of the internal tide. On the short time scale this is confined primarily to the surface layer. On the longer time scale it modifies the stratification along shelf slopes, and in particular those associated with off-shelf seamounts. The shelf slope modification is consistent with that found by XD97 using a cross sectional model. However, results from the present three-dimensional model show significant along slope variability, and the limitations of instrument deployments along a single cross section in terms of model validation.

4.2. *An up-welling favourable wind (wind towards the south)*

To determine the extent to which the internal tide is modified by an up-welling favourable wind stress, the previous calculations were repeated with a 0.2 Pa wind stress towards the south. Calculations were performed with both a short duration (Calc. 4) and longer duration (Calc. 5) wind stress.

With the short duration wind forcing, temperature contours along cross section D1n (not presented) show enhanced surface mixing, which was comparable to that found previously with the downwelling favourable wind. Some slight differences in the region of topographic slopes were evident due to changes in mixing with a down-welling wind compared to up-welling. The main features of the spatial distribution of the change in M_2 tidal current amplitude due to the up-welling wind (Fig. 9) are comparable to those found with the down-welling wind (Fig. 6). The most notable difference compared with the previous distribution (Fig. 6) is an increase in intensity and lateral extent in the surface region of difference in u current amplitude at about 10 °W. This is due to changes in shelf slope stratification which influences the generation region and subsequent propagation of the M_2 internal tide. At other cross sections (not shown) the change in the distribution of the

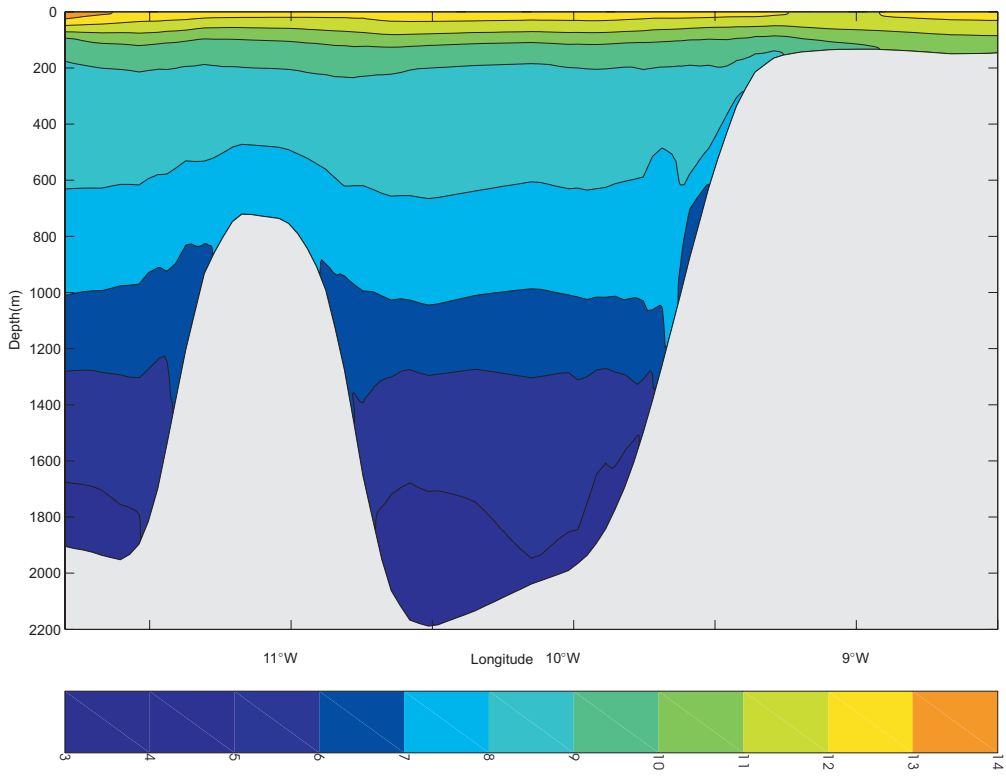

Fig. 7. Temperature contours (°C) at cross section D1n from a long tide and wind (0.2 Pa North) integration.

M_2 tidal current amplitude produced by wind forcing was comparable to that shown in Fig. 9.

For the calculation involving a longer duration 0.2 Pa wind (Calc. 5), there is appreciably more mixing in the slope regions. This is discussed in more detail in XD97 and will not be repeated here. Since this enhanced mixing occurs in the slope region and diffuses out of this area into the water column, it influences the regions where the internal tide is generated and its subsequent propagation. The enhanced mixing with the longer duration wind explains the increased differences in the pattern of change in the M_2 internal tide produced with a down-welling compared to up-welling favourable wind (compare Figs. 8 and 10). However, the dominant large-scale features are similar suggesting these are mainly determined by the topography. As previously this pattern of change is comparable at other cross sections in the region of the seamount, although qualitatively different.

These comparisons show that on the longer time scale there are appreciable differences in the change of the M_2 internal tide under down-welling compared to up-welling wind forcing. These differences arise not only in the surface layer but at depth where the wind field has modified the density field in the region of internal tide generation. This shows that not only is the internal tide modified in its generation region, but its propagation and subsequent reflection at the surface are influenced by wind mixing.

5. Concluding discussion

In this paper, a three dimensional finite element tidal model of the shelf edge region off the west coast of Scotland (HD05a) is extended to examine the influence of wind effects upon the M_2 internal tide in the area. The spatial variability of t.k.e. and associated mixing was also considered. Previous calculations (XD97) used a simple cross sectional finite difference model with idealized topography to study the influence of the wind. Such a slice model could not account for the along-shelf variation of topography, or for the presence of seamounts. As shown in HD05a, b, the finite element model with its ability to refine the grid in regions of rapid topographic change is an ideal tool to study topographic effects upon internal motions and hence extend the work of XD97.

In initial calculations, the model was forced with the same M_2 tidal distribution of the barotropic tide as in HD05a. However, the main focus of the present calculations was an examination of the spatial distribution of the internal tide. Theory, based upon idealized smooth topography and the absence of viscous effects, shows that internal wave energy propagates away from the generation site along characteristic surfaces, termed beams. However, the calculations presented here showed that with realistic topography and viscous effects there was no well-defined point for the M_2 tide generation or well defined beams along which

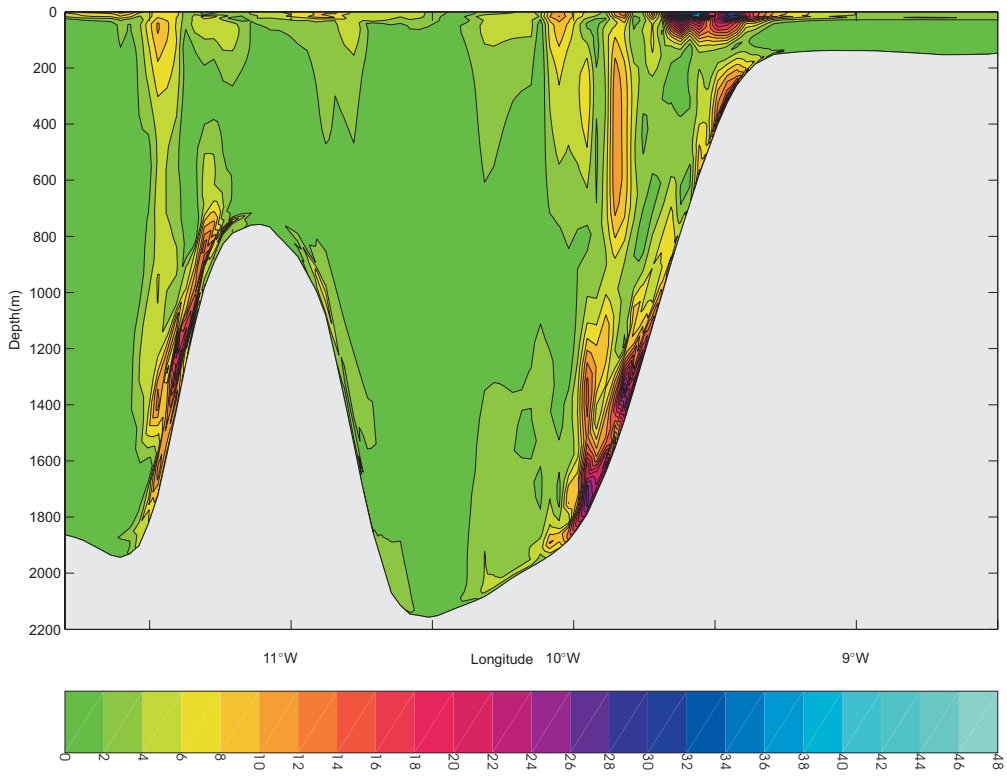

Fig. 8. As Fig. 6 but for a long integration (Calc. 3) with tide and wind (0.2 Pa North).

it propagated. This was rather different than the isolated seamount results of Lamb (2004) who showed narrow well defined beams for M_2 propagation.

These differences between narrow beams found with idealized topography and the weaker broader beams found with realistic topography with viscous effects included, in part reflects the additional complexity of the problem when realistic topography is included. Also in a three dimensional model in which the grid is refined in regions of steep topography, there may be a lack of resolution elsewhere. This combined with diffusive effects could lead to a spreading of internal tidal beams. Consequently, besides choosing the mesh to reflect topography and density variation, although it will give a fine mesh in the generation region, it is also necessary to preserve high resolution along the propagation pathways. As these are difficult to determine, then the choice of an optimum mesh, or an optimum measurement strategy is prone to significant uncertainty.

In addition, to the spatial variability of the internal tide, distributions of tidally induced t.k.e. were considered. The associated mixing gave rise to changes in the temperature field that were also examined. On the shelf strong tidal mixing led to a homogeneous water column, while in regions of steep topography the vertical displacement of isotherms due to tidal up-welling and down-welling gave regions of enhanced boundary layer mixing. The extent of this mixing increased with time in particular in the region of the seamount, where a pool of cooler water occurred above the seamount associated with enhanced mixing in the region. Increased tidally induced mixing above seamounts appears common and has been found elsewhere, e.g. the Fieberling Seamount (Kunze and Toole (1997)). A cold-water region also occurred along the shelf edge in the northern part of the region at a depth of 600m due to increased mixing in this area at this depth. The intensity and lateral extent of this cool water region could be related to variations in location and depth of internal tide generation with the associated t.k.e. production and elevated boundary layer mixing. Turbulent kinetic energy contours revealed significant spatial variability in turbulence, with regions of strong near bed turbulence associated with areas of enhanced M_2 internal tidal current.

Having determined the spatial distribution of the amplitude of the M_2 internal tidal currents and associated mixing in a subsequent series of calculations the influence of wind forcing upon them was examined. A wind stress of 0.2 Pa either towards the north (down-welling favourable) or towards the south (up-welling favourable) was applied. Initially a short duration wind was used, although subsequently a longer duration wind was applied.

On the short time scale the down-welling favourable wind only modified the near surface stratification, and the change to the M_2 internal tidal current was restricted to the surface layer. Areas of maximum modification of internal tidal

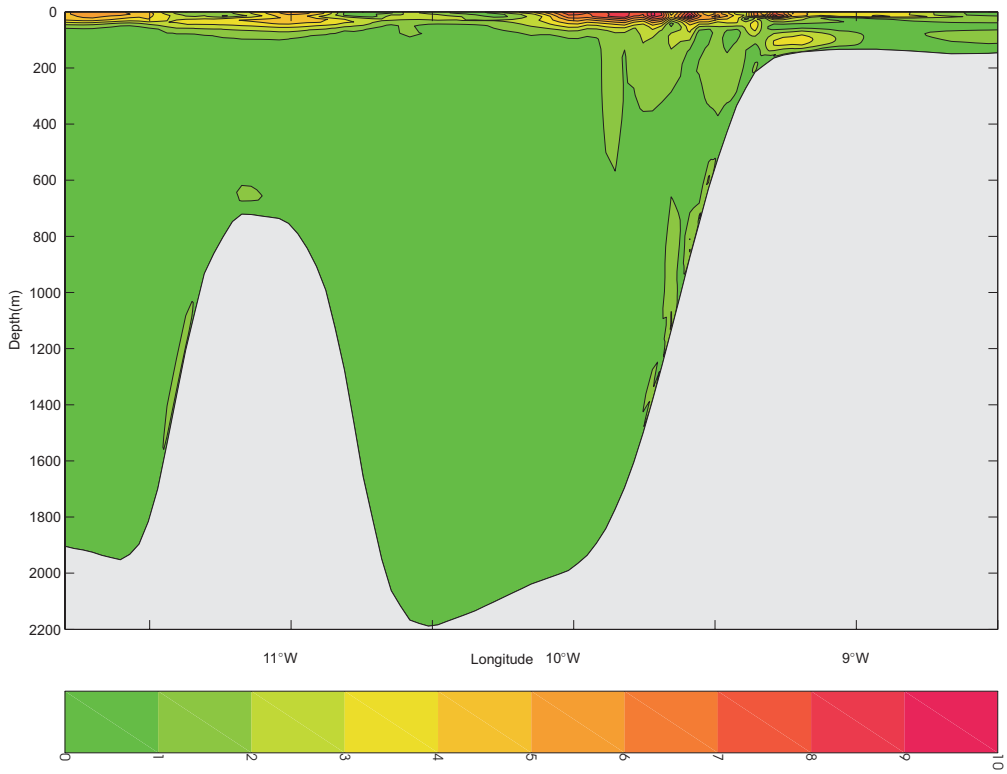

Fig. 9. Contours of the difference in baroclinic tidal current amplitude (cm s^{-1}) between wind (0.2 Pa South) and tidal solution and a tide only solution for short wind duration forcing (Calc. 4) at cross section D1n for the M_2 period.

current occurred in the surface layer above the seamount and shelf break, where the tidal current was a maximum. On the longer time scale both the tide and down-welling favourable wind modified the temperature field at depth, giving rise to a modification of the density field at depth and a change in the distribution of the internal tide. Associated with these changes in tidal distribution were modifications to the t.k.e. field.

Changes in the M_2 internal tide produced with up-welling favourable winds on the short time scale were comparable to those found with the downwelling favourable wind. The reason for this is that on the short time scale it is the mixing in the surface layer that has the greatest effect and this is not significantly influenced by wind direction. On the longer time scale there were differences in mixing in the slope regions between down-welling and upwelling favourable winds. These gave rise to an appreciable modification of the M_2 internal tide together with boundary layer turbulence. Although in practice a persistent wind from a given direction is unlikely to occur, these calculations do show that the internal tide is modified by density changes produced by the wind. In addition, changes in density field in the shelf edge region are likely to occur due to large scale modulation of the along shelf flow by oceanic effects. These will also lead to changes in the internal tide and associated t.k.e. levels and mixing.

The extent to which an along shelf flow of oceanic origin or produced by wind forcing can penetrate on to the shelf is determined by bottom frictional effects (e.g. Hill (1995)). Since the tidal flow in the shelf edge region and on the shelf determines the level of friction, it is essential to include it within any model of the wind induced circulation of the shelf edge region (e.g. Davies and Xing (2005b); Xing and Davies (1996b, 2001a)).

As we have shown in this paper, the fact that the distribution of the M_2 internal tide is particularly sensitive to topographic variations and density field has major implications for model validation and data collection. To enable the modelling of internal tides to progress to the same extent as that achieved for barotropic tides will require a way forward based on major observational and modelling programmes. In terms of topography a detailed measurement programme is required to produce high-resolution water depths in shelf edge regions. As found in a comprehensive and detailed comparison of observed and modelled internal tides in the region, using a range of grids (HD05a), although the model grid can be refined in the shelf edge region thereby improving resolution, there is a lack of detailed depth data to ensure that the finer resolution grid accurately reproduces the local topographic gradient. As known from theory the local topographic gradient is crucial for internal tide generation.

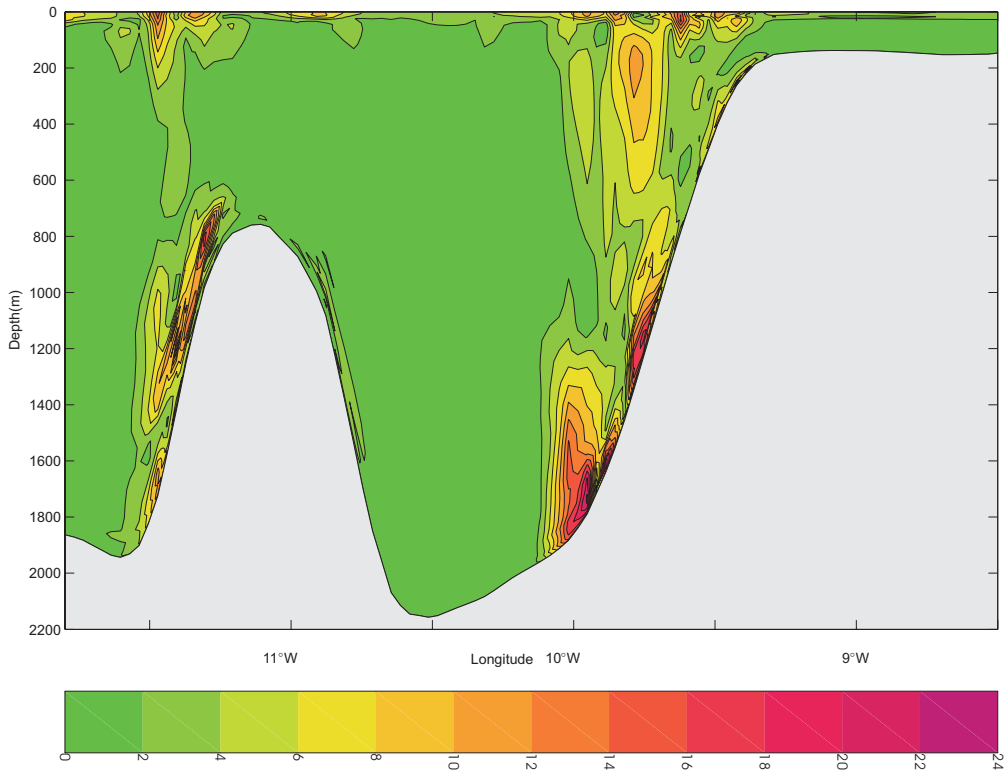

Fig. 10. As Fig. 9, but for a long duration wind (0.2 Pa South) (Calc. 5).

Since topographic measurements do not have to be taken at the same time, a piece-meal approach to developing a comprehensive topographic data set is possible. On the other hand a near synoptic data set of temperature and salinity is required to provide an initial density field for an internal tidal model. Theory and detailed comparisons with measurements (XD98, HD05a) have shown that internal tide generation and propagation is particularly sensitive to the density distribution at the time measurements are made.

As shown here meteorological effects can significantly influence density distributions and hence internal tide production and propagation in regions of abrupt topography. This suggests that detailed meteorological data at the time internal tide measurements are made is required in such areas. Away from topographic effects, and the surface thermocline where, as we have shown short term variations of mixing due to atmospheric forcing are likely to occur, the larger scale density field is more persistent and probably does not require high resolution sampling. However, the advection of oceanic water into a regional model would have to be monitored, together with more detailed measurements of temperature, salinity and mixing in regions of steep topography. These would be required to provide accurate initial conditions for the model and to check that the model was reproducing the correct density distribution in regions where the internal tide was generated. As shown here, the high degree of spatial variability of the internal tide from one cross section to another in areas of steep topography suggests that detailed measurements are required in these regions. In addition, the high degree of spatial variability found in t.k.e. intensity in regions of steep topography suggests that detailed measurements of turbulence dissipation rate and mixing are required in such areas. However, the persistence of enhanced mixing above topographic features such as the Anton Dohrn Seamount, with corresponding regions found elsewhere in the location of seamounts (e.g. the Fieberling Seamount (Kunze and Toole (1997))), suggests that these areas together with other regions of steep topography could be the focus of detailed measurements to validate mixing intensities computed with internal tidal models. The ability of an unstructured mesh model to focus resolution in these areas suggests that it is an ideal tool to use to complement the high-resolution measurements that will be required in these regions. In addition, to changes in density field influencing the propagation of internal waves, regions of lateral horizontal shear associated with fronts (Davies and Xing (2005a); Xing and Davies (2005)) also affect internal wave propagation and can lead to local enhanced mixing. Detailed measurements of lateral shear in such regions, and unstructured grid models with the ability to reproduce these shears is an essential feature of any long term internal tide prediction system. However, in terms of short term predictions, data assimilation methods (Ku-

rapov et al. (2003)) can be used to enhance model accuracy provided detailed measurements are available for assimilation.

The calculations described here were performed with a hydrostatic model. However, recent measurements (e.g. Inall et al. (2004, 2005)) and modelling (Xing and Davies (2006)) suggest that non-hydrostatic effects will be important in regions of steep topography. Such models are currently being developed using topography following coordinates (e.g. Berntsen and Furnes (2005); Heggelund et al. (2004); Berntsen et al. (2006)) or with a z-coordinate (Adcroft et al. (1997); Marshall et al. (1997a,b); Pain et al. (2005)). They have recently been used in a z-coordinate form (Legg (2004a,b)) to investigate internal tide generation at a shelf slope. Calculations show that the effect of including non-hydrostatic processes is to significantly enhance small-scale variability in the internal tide generation region. In addition, inclusion of non-hydrostatic effects permits soliton generation and propagation. A rigorous validation of a models ability to generate and propagate these small-scale features would require a major measurements programme, not only in their generation region but in the far field area into which they propagate.

Recent calculations (Xing and Davies (2006)) with small scale topography and non-hydrostatic models demonstrate that there is significant energy loss from the tide into small scale mixing processes in regions of rough topography such as the shelf slope. Basin scale calculations (Samelson (1998); Spall (2001); Saenko and Merrifield (2005); Saenko (2006)) have shown that the ocean circulation is influenced by these shelf edge mixing processes. The disparity in grid size between basin scale models (of order kilometres) and the small scale calculations of Xing and Davies (2006) (grid size of order meters) suggests that an important future topic will be using high resolution models to develop mixing parameterizations suitable for large scale models.

With present advances in computing, it is clear that three-dimensional models using unstructured grids and the inclusion of non-hydrostatic effects will replace the conventional uniform grid finite difference model in the near future. To parallel these developments major comprehensive measurement programmes will be required particularly in shelf edge regions where there are rapid changes in topography and associated small-scale variability. Improvements in the ability of shelf edge models to predict internal tidal distributions, and the associated small scale variations in currents, internal wave fields and mixing will have important consequences in sediment (e.g. Davies and Xing (2002); Xing and Davies (2002); Davies et al. (2002)) and biological modelling. In these models accurate and detailed descriptions of flow fields, associated mixing, internal wave fields and bed stresses are essential to progress the modelling of sediment and biological processes.

Acknowledgements

The authors are indebted to Mrs. L. Parry for typing the paper and Mr. R.A. Smith for help in figure production. Access to bottom topography, open boundary forcing were provided by Dr. J. Xing and are gratefully acknowledged. Access to the QUODDY code via the web site is much appreciated.

References

Adcroft, A., Hill, C., Marshall, J., 1997. Representation of topography by shaved cells in a height coordinate ocean model. Monthly Weather Review 125, 2293–2315.

Berntsen, J., Furnes, G. K., 2005. Internal pressure errors in sigma-coordinate ocean models—sensitivity of the growth of the flow to the time stepping method and possible nonhydrostatic effects. Continental Shelf Research 25, 829–848.

Berntsen, J., Xing, J., Alendal, G., 2006. Assessment of non-hydrostatic ocean models using laboratory scale problems. Continental Shelf Research 26, 1433–1447.

Blumberg, A. F., Mellor, G. L., 1987. A description of a three-dimensional coastal ocean circulation model. No. 4 in Coastal and Estuarine Sciences. American Geophysical Union, Washington, DC, p. 208pp.

Cartwright, D. E., 1976. Shelf edge tidal measurements between ireland and norway. Memoires de la Societe Royale des Sciences de Liege 10, 133–140.

Chen, P., Mellor, G. L., 1999. Determination of tidal boundary forcing using tide station data. No. 56 in Coastal and Estuarine Studies. American Geophysical Union, Washington, DC, pp. 329–351.

Craig, P. D., 1987. Solutions for internal tide generation over coastal topography. Journal of Marine Research 45, 83–105.

Cummins, P. F., Cherniawsky, J. Y., Foreman, M. G. G., 2001. North Pacific internal tides from the Aleutian Ridge: altimeter observations and modeling. Journal of Marine Research 59, 167–191.

Cummins, P. F., Oey, L. Y., 1997. Simulation of barotropic and baroclinic tides off Northern British Columbia. Journal of Physical Oceanography 27, 762–781.

Davies, A. M., Xing, J., 2002. Processes influencing suspended sediment movement on the Malin-Hebrides shelf. Continental Shelf Research 22 (15), 2081–2113.

Davies, A. M., Xing, J., 2005a. The effect of a bottom shelf front upon the generation and propagation of near-inertial internal waves in the coastal ocean. Journal of Physical Oceanography 35, 976–990.

Davies, A. M., Xing, J., 2005b. Modelling processes influencing shelf edge exchange of water and suspended sediment. Continental Shelf Research 25, 973–1001.

Davies, A. M., Xing, J., Huthnance, J. M., Hall, P., Thomsen, L., 2002. Models of near-bed dynamics and sediment movement at the Iberian margin. Progress in Oceanog-

raphy 52 (2-4), 373–397.
Egbert, G. D., Erofeeva, S. Y., 2002. Efficient inverse modeling of barotropic ocean tides. Journal of Atmospheric and Oceanic Technology 19, 183–204.
Flather, R. A., 1976. A tidal model of the north west European continental shelf. Memoires de la Societe Royale des Sciences de Liege 10, 141–164.
Flather, R. A., Hubbert, K. P., 1989. Tide and surge models for shallow water—Morecambe Bay revisited. Vol. 1. CRC Press, Boca Raton, FL, pp. 135–166.
Fortunato, A. B., Baptista, A. M., Luettich, R. A., 1997. A three-dimensional model of tidal currents in the mouth of the Tagus estuary. Continental Shelf Research 17, 1689–1714.
Fortunato, A. B., Oliviera, A., Baptista, A. M., 1999. On the effect of tidal flats on the hydrodynamics of the Tagus estuary. Oceanologica Acta 22, 31–44.
Gerkema, T., 2001. Internal and interfacial tides: beam scattering and local generation of solitary waves. Journal of Marine Research 59, 227–251.
Gerkema, T., 2002. Application of an internal tide generation model to baroclinic spring-neap cycles. Journal of Geophysical Research 107(C9), 3124.
Gerkema, T., Zimmerman, J. T. F., 1995. Generation of noni-linear internal tides and solitary waves. Journal of Physical Oceanography 25, 1081–1094.
Gjevik, B., Hareide, D., Lynge, B. K., Ommundsen, A., Skailand, J. H., Urheim, H. B., 2006. Implementation of high resolution tidal current fields in electric navigational chart systems. Marine Geodesy 29, 1–17.
Greenberg, D. A., Dupont, F., Lyard, F. H., Lynch, D. R., Werner, F. E., 2007. Resolution issues in numerical models of oceanic and coastal circulation. Continental Shelf Research 27, 1317–1343.
Hall, P., Davies, A. M., 2005a. Comparison of finite difference and element models of internal tides on the Malin-Hebrides shelf. Ocean Dynamics 55, 272–293.
Hall, P., Davies, A. M., 2005b. Effect of coastal boundary resolution and mixing upon internal wave generation and propagation in coastal regions. Ocean Dynamics 55, 248–271.
Hall, P., Davies, A. M., 2005c. The influence of an irregular grid upon internal wave propagation. Ocean Modelling 10, 193–209.
Haney, R. L., 1991. On the pressure gradient force over steep topography in sigma coordinate ocean models. Journal of Physical Oceanography 21, 610–619.
Heggelund, Y., Vikeb, F., Berntsen, J., Furnes, G. K., 2004. Hydrostatic and non-hydrostatic studies of gravitational adjustment over a slope. Continental Shelf Research 24, 2133–2148.
Heniche, M., Secretin, Y., Boudreau, P., Leclerc, M., 2000. A two-dimensional finite element drying-wetting shallow water model for rivers and estuaries. Advances in Water Resources 23, 359–372.
Hibiya, T., 2004. Internal wave generation by tidal flow over a continental shelf slope. Journal of Oceanography 60, 637–643.
Hill, A. E., 1995. Leakage of barotropic slope currents onto the continental shelf. Journal of Physical Oceanography 25, 1617–1621.
Holloway, P. E., 1996. A numerical model of internal tides with applications to the Australian North-West shelf. Journal of Physical Oceanography 26, 21–37.
Holloway, P. E., Merrifield, M. A., 1999. Internal tide generation by seamounts, ridges, and islands. Journal of Geophysical Research 104(C11), 25,937–25,951.
Inall, M. E., Cottier, F. R., Griffiths, C., Rippeth, T. P., 2004. Sill dynamics and energy transformation in a jet fjord. Ocean Dynamics 54, 307–314.
Inall, M. E., Rippeth, T. P., Griffiths, C., Wiles, P., 2005. Evolution and distribution of T.K.E. production and dissipation within stratified flow over topography. Geophysical Research Letters 32, L08607.
Ip, J. T. C., Lynch, D. R., Friedrichs, C. T., 1998. Simulation of estuarine flooding and dewatering with application to Great Bay, New Hampshire. Estuarine, Coastal and Shelf Science 47, 119–141.
Khatiwala, S., 2003. Generation of internal tides in an ocean of finite depth: analytical and numerical calculations. Deep-Sea Research I 50, 3–21.
Kunze, E., Toole, J. M., 1997. Tidally driven vorticity, diurnal shear, and turbulence atop Fieberling Seamount. Journal of Physical Oceanography 27, 2663–2693.
Kurapov, A. L., Egbert, G. D., Allen, J. S., Miller, R. N., Erofeeva, S. Y., Kosro, P. M., 2003. The m_2 internal tide off Oregon: Inferences from data assimilation. Journal of Physical Oceanography 33, 1733–1757.
Lamb, K. G., 1994. Numerical experiments of internal wave generation by strong tidal flow across a finite amplitude bank edge. Journal of Geophysical Research 99(C1), 843–864.
Lamb, K. G., 2002. A numerical investigation of solitary internal waves with trapped cores formed via shoaling. Journal of Fluid Mechanics 451, 109–144.
Lamb, K. G., 2004. Non-linear interaction among internal wave beams generated by tidal flow over supercritical topography. Geophysical Research Letters 31, L09313.
Lamb, K. G., 2007. Energy and pseudoenergy flux in the internal wave field generated by tidal flow over topography. Continental Shelf Research 27, 1208–1232.
Legg, S., 2004a. Internal tides generated on a corrugated continental slope. part ii. along-slope barotropic forcing. Journal of Physical Oceanography 34, 1824–1838.
Legg, S., 2004b. Internal tides generated on a corrugated slope. part i: Cross-slope barotropic forcing. Journal of Physical Oceanography 34, 156–173.
Legg, S., Adcroft, A., 2003. Internal wave breaking at concave and convex continental slopes. Journal of Physical Oceanography 33, 2224–2246.
Legrand, S., Deleersnijder, E., Delhez, E., Legat, V., 2007. Unstructured, anisotropic mesh generation for the Northwestern European continental shelf, the continental slope and the neighbouring ocean. Continental Shelf

Research 27, 1344–1356.

Luyten, P. J., Carniel, S., Umgiesser, G., 2002. Validation of turbulence closure parameterizations for stably stratified flows using the PROVESS turbulence measurements in the North Sea. Journal of Sea Research 47, 239–267.

Lynch, D., Hannah, C. G., 2001. Inverse model for limited-area hindcasts on the continental shelf. Journal of Atmospheric and Oceanic Technology 18, 962–981.

Lynch, D. R., Ip, J. T. C., Naimie, C. E., Werner, F. E., 1996. Comprehensive coastal circulation model with application to the Gulf of Maine. Continental Shelf Research 16, 875–906.

Lynch, D. R., Smith, K., Blanton, B., Luettich, R., Werner, F. E., 2004. Forecasting the coastal ocean: resolution, tide, and operational data in the South Atlantic Bight. Journal of Atmospheric and Oceanic Technology 21, 1074–1085.

Marshall, J., Hill, A. A. C., Perelman, L., Heisey, C., 1997a. A finite-volume incompressible Navier Stokes model for studies of the ocean on parallel computers. Journal of Geophysical Research 102, 5753–5766.

Marshall, J., Hill, C., Perelman, L., Adcroft, A., 1997b. Hydrostatic, quasi-hydrostatic and nonhydrostatic ocean modelling. Journal of Geophysical Research 102(C3), 5733–5752.

Mellor, G. L., Oey, L. Y., Ezer, T., 1998. Sigma coordinate pressure gradient errors and the seamount problem. Journal of Atmospheric and Oceanic Technology 15, 1122–1131.

Merrifield, M. A., Holloway, P. E., 2002. Model estimates of m_2 internal tide energetics at the Hawaiian Ridge. Journal of Geophysical Research 107(C8), 3179.

Munroe, J. R., Lamb, K. G., 2005. Topographic amplitude dependence of internal wave generation by tidal forcing over idealized three-dimensional topography. Journal of Geophysical Research 110, C02001.

New, A. L., 1988. Internal tidal mixing in the bay of biscay. Deep-Sea Research 35, 691–709.

Niwa, Y., Hibiya, T., 2004. Three-dimensional numerical simulation of m_2 internal tides in the East China Sea. Journal of Geophysical Research 109, C04027.

Pain, C. C., Piggott, M. D., Goddard, A. J. H., Fang, F., Gorman, G. J., Marshall, D. P., Eaton, M. D., Power, P. W., de Oliveira, C. R. E., 2005. Three-dimensional unstructured mesh ocean modelling. Ocean Modelling 10, 5–33.

Pingree, R. D., New, A. L., 1989. Downward propagation of internal tidal energy into the Bay of Biscay. Deep-Sea Research 36, 735–758.

Pingree, R. D., New, A. L., 1991. Abyssal penetration and bottom reflection of internal tidal energy into the Bay of Biscay. Journal of Physical Oceanography 21, 28–39.

Pingree, R. D., New, A. L., 1995. Structure, seasonal development and sunglint spatial coherence of the internal tide on the Celtic and Armorican shelves in the Bay of Biscay. Deep-Sea Research I 42, 245–284.

Proctor, R., James, I. D., 1996. A fine-resolution 3D model of the southern North Sea. Journal of Marine Systems 8, 285–295.

Saenko, O. A., 2006. The effect of localized mixing on the ocean circulation and time-dependent climate change. Journal of Physical Oceanography 36, 140–160.

Saenko, O. A., Merrifield, W. J., 2005. On the effect of topographically enhanced mixing on the global ocean circulation. Journal of Physical Oceanography 35, 826–834.

Samelson, R. M., 1998. Large scale circulation with locally enhanced vertical mixing. Journal of Physical Oceanography 28, 712–726.

Sherwin, T. J., Taylor, N. K., 1989. The application of a finite difference model of internal tide generation to the NW European Shelf. Deutsche Hydrographische Zeitschrift 42, 151–167.

Sherwin, T. J., Taylor, N. K., 1990. Numerical investigations of linear internal tide generation in the Rockall Trough. Deep-Sea Research 37, 1595–1618.

Sherwin, T. J., Vlasenko, V. I., Stashchuk, N., Jeans, D. R. G., Jones, B., 2002. Along-slope generation as an explanation for some unusually large internal tides. Deep-Sea Research I 49, 1787–1799.

Shum, C. K., Woodworth, P. L., Andersen, O. B., Egbert, G. D., Francis, O., King, C., Klosko, S. M., le Provost, C., Li, X., Molines, J. M., Parke, M. E., Ray, R. D., Schlax, M. G., Stammer, D., Tierney, C. C., Vincent, P., Wunsch, C. I., 1997. Accuracy assessment of recent ocean tide models. Journal of Geophysical Research 102(C11), 25,173–25,194.

Simmons, H. L., Hallberg, R. W., Arbic, B. K., 2004. Internal wave generation in a global baroclinic tide model. Deep-Sea Research II 51, 3043–3068.

Smagorinsky, J., 1963. General circulation experiments with the primitive equations I. The basic experiment. Monthly Weather Review 91, 99–164.

Spall, M. A., 2001. Large scale circulations forced by localized mixing over a sloping bottom. Journal of Physical Oceanography 31, 2369–2384.

St. Laurent, L., Stringer, S., Garrett, C., Perrault-Joncas, D., 2003. The generation of internal tides at abrupt topography. Deep-Sea Research I 50, 987–1003.

Thompson, K. R., Griffin, D. A., 1998. A model of the circulation on the outer Scotian Shelf with open boundary conditions inferred by data assimilation. Journal of Geophysical Research 103(C13), 30,641–30,660.

Thompson, K. R., Ohashi, K., Sheng, J., Bobanovic, J., Ou, J., 2007. Suppressing bias and drift of coastal circulation models through the assimilation of seasonal climatologies of temperature and salinity. Continental Shelf Research 27, 1303–1316.

Walters, R. A., 1987. A model for tides and currents in the English Channel and North Sea. Advances in Water Resources 10, 138–148.

Walters, R. A., 2005. Coastal ocean models: two useful finite element methods. Continental Shelf Research 25, 775–794.

Walters, R. A., Werner, F. E., 1989. A comparison of two

finite element models of tidal hydrodynamics using a North Sea data set. Advances in Water Resources 12, 184–193.

Werner, F. E., 1995. A field test case for tidally forced flows: a review of the tidal flow forum. American Geophysical Union, Washington, DC, pp. 269–284.

Xing, J., Davies, A. M., 1996a. Application of turbulence energy models to the computation of tidal currents and mixing intensities in shelf edge regions. Journal of Physical Oceanography 26, 417–447.

Xing, J., Davies, A. M., 1996b. A numerical model of the long term flow along the Malin-Hebrides shelf. Journal of Marine Systems 8(304), 191–218.

Xing, J., Davies, A. M., 1996c. Processes influencing the internal tide, its higher harmonics, and tidally induced mixing on the Malin-Hebrides shelf. Progress in Oceanography 38, 155–204.

Xing, J., Davies, A. M., 1997a. Application of a range of turbulence energy models to the computation of the internal tide. International Journal of Numerical Methods in Fluids 26, 1055–1084.

Xing, J., Davies, A. M., 1997b. The influence of wind effects upon internal tides in shelf edge regions. Journal of Physical Oceanography 27, 205–262.

Xing, J., Davies, A. M., 1998a. Influence of stratification upon diurnal tidal currents in shelf edge regions. Journal of Physical Oceanography 28(9), 1803–1831.

Xing, J., Davies, A. M., 1998b. A three-dimensional model of internal tides on the Malin-Hebrides shelf and shelf edge. Journal of Geophysical Research 103(C) (12), 27821–27847.

Xing, J., Davies, A. M., 1999. The influence of topographic features and density variations upon the internal tides in shelf edge regions. International Journal of Numerical Methods in Fluids 31, 535–577.

Xing, J., Davies, A. M., 2001a. The influence of shelf edge flows and wind upon the circulation on the Malin Shelf and in the Irish Sea. Continental Shelf Research 21(1), 21–45.

Xing, J., Davies, A. M., 2001b. Non-linear effects of internal tides on the generation of the tidal mean flow at the Hebrides shelf edge. Geophysical Research Letters 28, 3939–3942.

Xing, J., Davies, A. M., 2001c. A three-dimensional baroclinic model of the Irish Sea: Formation of the thermal fronts and associated circulation. Journal of Physical Oceanography 31, 94–114.

Xing, J., Davies, A. M., 2002. Influence of wind direction, wind waves and density stratification upon sediment transport in shelf edge regions: Iberian Shelf. Journal of Geophysical Research 107(C8), 16–1–16–24.

Xing, J., Davies, A. M., 2005. Influence of a cold water bottom dome on internal wave trapping. Geophysical Research Letters 32, L03601, doi:10.1029/2004GLO21833.

Xing, J., Davies, A. M., 2006. Processes influencing tidal mixing in the region of sills. Geophysical Research Letters 33, L04603.